Discussion on "Dynamic soil-structure interaction: A three-dimensional numerical approach and its application to the Lotung case study". Poor performance of the HSS model

A. Niemunis

Institute of Soil Mechanics and Rock Mechanics,

Karlsruhe Institute of Technology, Germany,

e-mail: Andrzej.Niemunis@kit.edu

M. Cudny

Department of Geotechnics, Geology and Marine Civil Engineering,

Faculty of Civil and Environmental Engineering,

Gdańsk University of Technology, Poland,

corresponding author, e-mail: mcud@pg.gda.pl

February 21, 2018

Postprint of: Niemunis A., Cudny M.: Discussion on "Dynamic soil-structure interaction: A three-dimensional numerical approach and its application to the Lotung case study". Poor performance of the HSS model. COMPUTERS AND GEOTECHNICS. Vol. 98, (2018), p. 243-245. DOI: 10.1016/j.compgeo.2018.02.003

1 Introduction

The authors of [1] present an interesting analysis of dynamic soil-structure interaction with references and validation to the records from the Lotung large-scale seismic test site. In the numerical calculations they use the commercial FE code Plaxis [5] with the Hardening Soil Small (HSS) constitutive model. The authors claim that a satisfactory agreement is achieved between the experimental and numerical results. However, usage of the HSS model may in general lead to a significant error known as overshooting. In particular, the problem may appear during a predominantly monotonic deformation interrupted by an occasional small unloading-reloading cycle (e.g. due to a dynamic disturbance).

Admittedly, we use this discussion of [1] as the opportunity to present the overshooting problem in the HSS and this discussion may be of more general interest. The HSS model originates from the elastoplastic Hardening Soil (HS) model by Schanz [12]. It was extended for small-strain stiffness by Benz [3, 4] and implemented into Plaxis FE code [5]. As a part of Plaxis the popularity of HSS is growing in geotechnical community. Being aware of this popularity of the HSS [1, 2, 7, 11, 13, 14] we decided to report on the overshooting.

The small-strain extension [3,4] was meant to improve the behaviour of the model making the reloading stiffer than the first loading. The main source of errors is related to the instantaneous decay of the history tensor $\mathbf{H}$ upon some even infinitesimally small strain increments. The consequences seem to have been overlooked so far.

The HSS is claimed to be paraelastic in [1]. The authors cite this claim after [3] without due scrutiny. Actually, the model is not paraelastic according to the definition in [3]. We may obtain accumulation of stress upon closed strain cycles (or vice versa) despite the fact that the loop starts and ends at a reversal point. Even the 1D version of the HSS is not paraelastic, let alone the full tensorial formulation. The HSS definition of the reversal point is a source of additional complication here. Actually, one can distinguish three different kinds of a reversal point depending on a comparison of non-coaxial tensors (see the next section). Besides, we do not recommend to classify the HSS as an "overlay model" because there is no parallel coupling of different materials, neither in the computation nor in the derivation of the model.

In the following text the naming conventions used by Benz [3] are preserved. The numbers of the original equations from [3] are written as (B6.x). In order to understand all technical details of this discussion readers are advised to have [3] at hand.

2 History tensor

The evolution of history tensor **H** proposed in [3] is rather unusual for elastoplastic models because it is driven by the total strain increments instead of the plastic ones. Hence, formally speaking, **H** is not a hardening parameter and it can be affected even by infinitesimally small elastic strain increments.

First, the deviatoric portion $\Delta e_{mn} = \Delta\varepsilon_{mn} - \delta_{mn}\Delta\varepsilon_{kk}$ of strain increment $\Delta\varepsilon_{mn}$ is diagonalized

$$\underline{\Delta\mathbf{e}} = \mathbf{S}\cdot\Delta\mathbf{e}\cdot\mathbf{S}^T \quad \text{or} \quad \underline{\Delta e}_{kl} = S_{km}\Delta e_{mn}S_{ln} \tag{1}$$

obtaining the eigenvalues $\underline{\Delta e}_{kl} = \ \mathrm{diag}(\underline{\Delta e}^1, \underline{\Delta e}^2, \underline{\Delta e}^3)$, where S_{ln} consists of the orthonormalized eigenvectors of the strain increment, as rows of the matrix **S**.

The history of strain H_{ij} is proposed to be of the second rank. Roughly speaking, small H_{ij} means increased stiffness. Tensor H_{ij} is initialized with zero components. In Appendix A of [3] on page. 168 we find the initialization[1] of $W_{ij} = \delta_{ij} + H_{ij}$ denoted in the code as `Hist1` in the form

$$W^0_{ij} = \delta_{ij} + H^0_{ij} = \delta_{ij} \tag{2}$$

in agreement with the Box (B6.1) on page 67, wherein $H^0_{ij} = 0$. In general, H_{mn} and Δe_{mn} are not coaxial. Hence, the transformation (B6.3), i.e.

$$\underline{H}_{kl} = S_{km}H_{mn}S_{ln} \tag{3}$$

with S_{ln} from (1) typically leaves some non-zero off-diagonal components[2]. The components on the

[1] The original implementation code sets $W_{ij} = 100\ \delta_{ij}$, because strain increments are presumably in [%]

[2] Comparing (3) with (B6.3) or (1) with (B6.2) we note that the transposition is missing in the original text. The error (omission of transposition) is absent in the FORTRAN implementation

diagonal of $\underline{H}_{kl}$ i.e. $\underline{H}_{11}, \underline{H}_{22}, \underline{H}_{33}$ are stored as `chi(1,:)` in the FORTRAN code[3]. For the evolution of $\underline{H}_{kl}$ Benz defines a diagonal so-called transformation matrix $\underline{T}_{km} =$ diag$(\underline{T}_{11}, \underline{T}_{22}, \underline{T}_{33})$ with

$$\underline{T}_{11} = \frac{1}{\sqrt{W_{11}}}\left[1 + h(\underline{\Delta e}^1 \underline{H}_{11})(\sqrt{W_{11}} - 1)\right] \quad \text{with} \quad W_{11} = 1 + \underline{H}_{11}\,, \tag{4}$$

$$\text{and analogously:} \quad \underline{T}_{22} = \ldots, \underline{T}_{33} = \ldots, \tag{5}$$

where $h(\sqcup) = \frac{1}{2}(1 + \text{sign}(\sqcup))$ is the Heaviside function. In particular[4] (a): $T_{11} = 1$ if $\underline{\Delta e}^1 \underline{H}_{11} \geq 0$ and (b): $T_{11} = 1/\sqrt{W_{11}}$ if $\underline{\Delta e}^1 \underline{H}_{11} < 0$. Judging by the FORTRAN code (line 131) the update of the history tensor from time $t^{(i)}$ to $t^{(i+1)}$ is calculated as

$$\underline{H}_{kl}^{(i+1)} + \delta_{kl} = \underline{T}_{km}\left(\underline{H}_{mn}^{(i)} + \delta_{mn}\right)\underline{T}_{nl} + \underline{\Delta e}_{kl} \tag{6}$$

in agreement with Box B.6.1 on page 67 but not with (B6.6). The transformation (6) applies to all components of $\underline{H}_{mn}^{(i)}$ and not just to the diagonal ones. After transformation (6) the "diagonalization" must be undone, viz.

$$H_{kl}^{(i+1)} = S_{mk}\underline{H}_{mn}^{(i+1)} S_{nl} \tag{7}$$

using the same matrix S_{ij} as in (3) but with different multiplications. A reversal point of the strain path is defined when the product $\underline{\Delta e}^i \underline{H}_{ii}$ (no sum over i) for any $i = 1, 2, 3$ is negative. After the update (6) both $\underline{H}_{kl}^{(i+1)} + \delta_{kl}$ and $\underline{\Delta e}_{kl}$ are diagonal. A scalar strain measure is defined by the product (B6.7), i.e.

$$\gamma_{\text{Hist}} = \sqrt{3}\|\underline{\Delta e}_{km}\underline{H}_{ml}^{(i+1)}\| \;/\; \|\underline{\Delta e}_{kl}\| \tag{8}$$

It is slightly inconsistent with the FORTRAN code (lines 137-140 p. 169). The code calculates a different

[3]Note that the eigenvectors in matrix `Trafo` are columns and not in rows. Besides, lines 98-111 of the code could be nicely abbreviated as `Hist2 = matmul( Transpose( Trafo), matmul( Hist1 , Trafo) )` in FORTRAN 90

[4]FORTRAN code on page 169, lines 113-124

norm, viz. $\|\underline{\Delta e}_{km}\underline{\hat{H}}^{(i+1)}_{ml}\| \neq \|\underline{\Delta e}_{km}\underline{H}^{(i+1)}_{ml}\|$ using just the diagonal components $\underline{\hat{H}}^{(i+1)}_{ml}$ from $\underline{H}^{(i+1)}_{ml}$. The secant stiffness

$$G = \frac{G_0}{1 + a\gamma_{\text{Hist}}/\gamma_{0.7}} \tag{9}$$

is large if γ_{Hist} is small. The material constants are G_0, a and $\gamma_{0.7}$.

Summing up, the deviatoric strain increment $\Delta\mathbf{e}$ is diagonalised using rotation matrix $\mathbf{S}$. The history $\mathbf{H}$ is rotated with the same $\mathbf{S}$ but $\mathbf{H}$ is not coaxial with $\Delta\mathbf{e}$ and hence $\mathbf{S}\cdot\mathbf{H}\cdot\mathbf{S}^T$ is not diagonal. Wherever the diagonal components of rotated matrices have opposite signs the history component is set to zero. Next, three products of diagonal components $p_i = \underline{\Delta e}^i\underline{H}_{ii}$ (no sum) are arranged in a vector (p_1, p_2, p_2). Its length $\gamma_{\text{Hist}}/\sqrt{3}$ is used to reduce the stiffness, viz. (9). After such modification the history is superposed by the diagonalized strain increment and then unrotated.

3 Overshooting

Let us consider a state with $\mathbf{H} \neq \mathbf{0}$ accumulated upon a long monotonic strain path. Suppose, we interrupt this path by an infinitesimally small disturbance. We choose it to be a small strain increment $\Delta\mathbf{e}$ coaxial with $\mathbf{H}$ and directed roughly towards $-\mathbf{H}$. In such case no rotation is required and since all diagonal components of $\Delta\mathbf{e}$ and $\mathbf{H}$ have opposite signs the HSS evolution rule renders $\mathbf{H} = \mathbf{0}$. Hence, even a single, infinitesimally small disturbance of the strain path may completely erase $\mathbf{H}$. This may strongly increase stiffness for all subsequent increments, here the continuation of the monotonic loading, see Figure 1. In the literature this problem is known as *overshooting* and it appears in numerous constitutive models. In particular, overshooting occurs in the hypoplastic model with the intergranular strain [8] (IS). However, we observe it first after a considerable number of small strain cycles which constitute a small elastic range. This effect is physically observed as a *shake-down*. In the small-strain paraelastic model [9, 10] (a revised version of the model by Hueckel and Nova [6]) the difficulties with overshooting have been overcome.

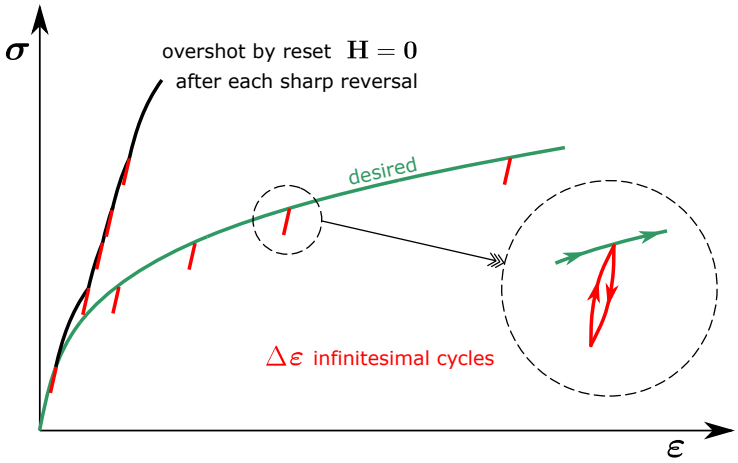

Figure 1: *The overshooting caused by an infinitesimally small unloading-reloading cycle (red). One can find various infinitesimal unloadings after which an arbitrary history tensor* $\mathbf{H}$ *vanishes completely.*

4 Incorrect response of the HSS obtained with PLAXIS

One can easily reproduce the above mentioned problems using the original implementation of the HSS model in the latest version of the PLAXIS FE code [5]. The element test of drained triaxial compression of initially overconsolidated soil has been chosen as an illustration.

The following set of material constants are taken from [3] :

$E_{50}^{\mathrm{ref}} = 8500\,\mathrm{kPa}$, $E_{oed}^{\mathrm{ref}} = 6150\,\mathrm{kPa}$, $E_{ur}^{\mathrm{ref}} = 25750\,\mathrm{kPa}$, $m = 0.7$, $c' = 6\,\mathrm{kPa}$, $\phi' = 28°$, $\psi = 0°$, $\gamma_{0.7} = 3.0 \cdot 10^{-4}$, $G_0^{\mathrm{ref}} = 60000\,\mathrm{kPa}$, $\nu_{ur} = 0.29$, $p_{\mathrm{ref}} = 100\,\mathrm{kPa}$.

The FE model for axisymmetric element tests (stress and strain fields are homogeneous) of dimensions 1×1m is meshed with 2 triangular elements. The vertical displacements at the bottom are fixed and the standard horizontal fixities at the symmetry line are applied. The uniform loading is controlled separately on the top and right sides of the sample (axial σ_a and radial σ_r stress components respectively). The soil is weightless and small initial isotropic stress ($p = 1\,\mathrm{kPa}$) is applied. The initial overconsolidation is set by the pre-overburden pressure ($POP = 100\,\mathrm{kPa}$) which results in preconsolidation pressure $p_p = 83.3\,\mathrm{kPa}$. The initial small strains are set to zero (the initial history tensor $\mathbf{H}$ is zero).

First, the soil is isotropically consolidated by applying the same axial and radial loading $\sigma_a = \sigma_r = -p_0 = -50\,\mathrm{kPa}$. Next, the soil is axially compressed under drained conditions keeping the radial stress $\sigma_r = \mathrm{const}$.

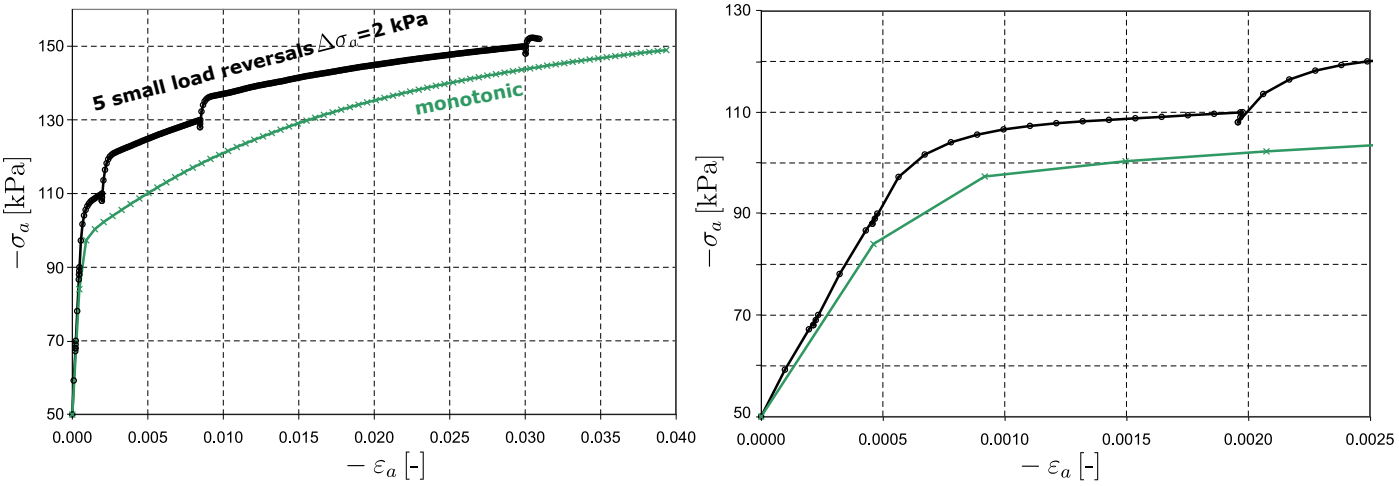

Figure 2: *Left: the overshooting calculated with the HSS model in the triaxial compression curve caused by 5 mini unloading-reloading cycles. Right: the first 2‰ of the axial deformation.*

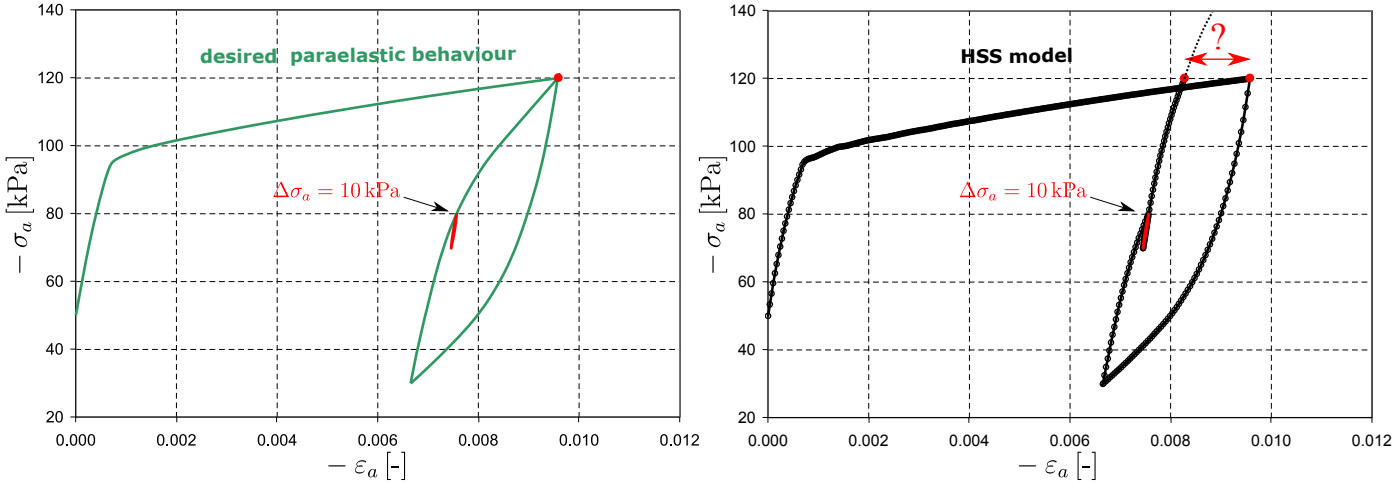

Figure 3: *Some hysteretic loops cannot be reproduced by the HSS model. The obtained response is not closed in strain.*

In the first calculation we demonstrate a typical numerical overshooting due to small-unloading reloading cycles during monotonic triaxial compression. Two stress-strain curves, both from HSS calculations, are compared in Figure 2:

- a monotonic increase of $\sigma_a(t)$ calculated as the reference - the lower curve,
- a non-monotonic increase, of $\sigma_a(t)$ with 5 small unloading-reloading cycles $\Delta\sigma_a = 2.0\,\mathrm{kPa}$, applied after reaching the level of every following 20 kPa up to shear failure - the upper curve.

The overshooting produced by the HSS upon non-monotonic loading is evident and consistent with the evolution of the history tensor $\mathbf{H}$ analysed in the discussion.

In the next calculation the HSS model is shown to violate the declared paraelastic behaviour. The numerical element test is performed with the same parameters set and with identical initial conditions. Starting from the isotropic consolidation $p_0 = 50\,\text{kPa}$ the axial stress reaches $\sigma_a = -120$ kPa followed by unloading to $\sigma_a = -30$ kPa and reloading back to $\sigma_a = -120$ kPa. If the reloading is interrupted by a mini unloading-reloading loop (here with $\Delta\sigma_a = 10\,\text{kPa}$ at $\sigma_a \approx -80\,\text{kPa}$) then the hysteretic loop is not closed at $\sigma_a = -120$ kPa, see Figure 3. A truly paraelastic model should respond with a closed $\varepsilon_a - \sigma_a$ loop despite the mini sub-cycle.

References

[1] A. Amorosi, D. Boldini, and A. di Lernia. Dynamic soil-structure interaction: A three-dimensional numerical approach and its application to the Lotung case study. Computers and Geotechnics, 90:34–54, 2017.

[2] A.A. Bagbag, B.M. Lehane, and J.P. Doherty. Predictions of footing and pressuremeter response in sand using a hardening soil model. Proceedings of the Institution of Civil Engineers - Geotechnical Engineering, 170(6):479–492, 2017.

[3] T. Benz. Small-strain stiffness of soils and its numerical consequences. PhD thesis, University of Stuttgart, 2007.

[4] T. Benz, P.A. Vermeer, and R. Schwab. A small-strain overlay model. International Journal for Numerical and Analytical Methods in Geomechanics, 33:25–44, 2009.

[5] R.B.J. Brinkgreve, S. Kumarswamy, and W.M. Swolfs. Material Models Manual. Plaxis BV, Delft, the Netherlands, 2017.

[6] T. Hueckel and R. Nova. Some hysteresis effects of the behaviour of geologic media. International Journal of Solids and Structures, 15:625–642, 1979.

[7] A. Ladesma and E.E. Alonso. Protecting sensitive constructions from tunnelling: the case of world heritage buildings in barcelona. Géotechnique, 67(10):914–925, 2017.

[8] A. Niemunis and I. Herle. Hypoplastic model for cohesionless soils with elastic strain range. Mechanics of Cohesive-Frictional Materials, 2:279–299, 1997.

[9] A. Niemunis, L. F. Prada-Sarmiento, and C. E. Grandas-Tavera. Extended paraelasticity and its application to a boundary value problem . Acta Geotechnica, 6(2):81–92, 2011.

[10] A. Niemunis, L. F. Prada-Sarmiento, and C. E. Grandas-Tavera. Paraelasticity. Acta Geotechnica, 6(2):67–80, 2011.

[11] A. Paternesi, H.F. Schweiger, and G. Scarpelli. Numerical analyses of stability and deformation behavior of reinforced and unreinforced tunnel faces. Computers and Geotechnics, 88:256–266, 2017.

[12] T. Schanz, P. A. Vermeer, and P. G. Bonnier. The hardening soil model: Formulation and verification. In Beyond 2000 in Computational Geotechnics - 10 Years of Plaxis. Balkema: Rotterdam, 1999.

[13] M. Shakeel and Charles W.W. Ng. Settlement and load transfer mechanism of a pile group adjacent to a deep excavation in soft clay. Computers and Geotechnics, In Press, Corrected Proof, 2017.

[14] P. Skels and K. Bondars. Applicability of small strain stiffness parameters for pile settlement calculation. Procedia Engineering, 172:999–1006, 2017.